Raman-scattering investigation of anharmonicity in potassium halides. Experiment and theory*

J. A. Taylor, M. S. Haque, J. E. Potts,† J. B. Page, Jr., and C. T. Walker
Department of Physics, Arizona State University, Tempe, Arizona 85281
(Received 13 August 1975)

Raman spectra of Tl^+-doped KCl, KBr, and KI have been measured as functions of hydrostatic pressure up to 7 kbar at 30, 85, and 300 K, and as functions of temperature at zero pressure. The data were analyzed using pure crystal p-V, bulk modulus, and thermal-expansion data. Calculations of the spectra have been performed using unperturbed or very weakly perturbed pure-crystal phonons and host bulk anharmonicity. Calculated shifts of prominent features in the impurity-induced E_g and T_{2g} spectra are found to be in good agreement with experiment. In all cases, the peak shifts can be accounted for by considering the volume dependence of phonon frequencies. The net contribution to peak shifts from multiphonon effects appears to be negligible.

I. INTRODUCTION

Because of their inherent structural simplicity, alkali halides have long been a favored system for experimental and theoretical studies of the lattice dynamics of crystals. Experiments in which these crystals are probed by Raman scattering have been hindered by selection rules which forbid first-order scattering, permitting only a weak, continuous, and complex second-order spectrum to be observed. However, the introduction of a substitutional impurity into the lattice lowers the symmetry at all lattice points except the defect site. The relaxed selection rules then permit the observation of a continuous first-order Raman spectrum with contributions from phonons throughout the Brillouin zone; inversion symmetry at the impurity site limits the Raman-active modes to symmetry types of even parity (A_{1g}, E_g, T_{2g}) in which the impurity remains at rest. The resultant impurity-induced spectrum is thus a measure of the perturbed crystal's density of states projected onto the even-parity modes. Since the Raman-active modes involve no motion of the defect, their frequencies and amplitudes will not be dependent on the impurity mass, but only on the force constants in the perturbed crystal. In an earlier study, Harley, Page, and Walker[1] (HPW) have shown that the introduction of Tl^+ impurity ions into potassium halide lattices has little or no influence on the lattice dynamics of the pure crystal. They found that, for KBr and KI, good agreement could be obtained between the measured helium-temperature spectrum and a 0-K calculation by assuming that the Tl^+ ion produced no change in the longitudinal overlap force constants between the defect and its nearest neighbors. For KCl, a 10% stiffening of the force constants was necessary to produce comparable agreement. The Tl^+ thus acts as an isotopic defect (or nearly so) whose sole effect is to induce the first-order Raman spectrum while having little or no influence on the lattice dynamics of the crystal. It is clearly of interest to exploit the power of this technique by studying these systems under the influence of external perturbations. We report here on our studies of anharmonicity in KCl, KBr, and KI via the temperature and hydrostatic pressure variations of the induced first-order spectra in Tl^+-doped crystals.[2]

Peaks in the induced first-order Raman spectrum result from contributions by many phonons throughout the Brillouin zone. Frequency shifts and broadening of these features are expected to result from two causes. First, as the volume of the unit cell changes, the harmonic force constants will assume new values appropriate to this new volume, resulting in a shift of the phonon frequencies. Second, anharmonic terms in the crystal potential will cause a coupling between phonons, leading to additional frequency shifts. It is possible to separate the volume and multiphonon contributions experimentally by performing a series of measurements. Frequency shifts measured as a function of temperature at constant pressure will contain contributions from both effects. On the other hand, the pressure dependence of the frequency shifts at liquid-helium temperatures (essentially 0 K for the purposes of comparison with theory) should reflect the volume change only. Therefore, by combining pressure dependence measurements at constant temperature with temperature-dependence measurements at constant (zero) pressure we have been able to determine the magnitudes of the volume and multiphonon contributions separately.

We have compared our measured spectra and frequency shifts with those calculated using the method described in HPW. Spectra were calculated within a quasiharmonic approximation using volume-dependent host-crystal phonons.

In Sec. II of this paper we describe the experi-

mental procedures and the methods of data reduction, and we display our results. Low-temperature spectra are shown and the spectral features which are to be followed in detail are identified. The volume dependence of these features, as deduced from all measurements as well as from theory, is also displayed. Section IV describes the methods used to calculate the volume-dependent spectra and presents comparisons between the measured and calculated spectra. In Sec. V we summarize our results and conclusions.

II. EXPERIMENT

Raman spectra were taken using the conventional 90° scattering geometry. A Spectra-Physics argon laser was operated at 514.5 nm with output power in the range 1–1.5 W. Scattered light was analyzed using Spex double monochromator with an ITT FW-130 cooled photomultiplier tube and SSR (now PAR) counting electronics. The observed spectra had rather different strengths, depending on host material, temperatures, symmetry studied, etc. Thus, the monochromator slits were adjusted so that the signal-to-noise ratios were roughly comparable from run to run, while keeping spectrum collection times reasonable. This resulted in varying resolutions, extending down to 2 cm^{-1} for very strong spectra and up to 6 cm^{-1} for very weak spectra. A polarization rotator on the front of the laser controlled the direction of polarization of the incident light while a polaroid sheet between the sample and the entrance slits of the monochromator allowed selection of the scattered light's polarization. As shown in HPW, only E_g and T_{2g} spectra are significant for Tl^+-doped alkali halides, so only these spectra were studied. The appropriate combinations of propagation directions and polarizations for the different symmetries are given in HPW.

Pressure-dependent Raman spectra were obtained using pressure-generating equipment of a standard design. Samples were mounted in a pressure vessel similar to the one reported by Fitchen.[3] The system used helium gas as the medium to transmit the hydrostatic pressure, and while the sample chamber was designed for maximum pressures of 10 kbar it was never operated above 7 kbar in order to prevent catastrophic breakdowns.

Pressure experiments at low temperatures were done by mounting the pressure cell on the cold finger of an optical cryostat. The helium gas was led into the cell by very-small-diameter stainless-steel tubing (o.d., 0.062 in; i.d., 0.007 in.) in order to minimize heat leaks. The pressure vessel leaked below 1.4 kbar, spoiling the vacuum in the cryostat. For this reason, low-temperature pressure runs were always done above 1.4 kbar. When the sample chamber was in the helium temperature range the helium transmitting gas froze, necessitating use of standard methods[4] for correcting the pressure. More seriously, in order to change the pressure it was necessary to warm the entire sample chamber until the helium melted. The pressure was then changed to a new value and the chamber recooled. This procedure resulted in the copious use of liquid helium. A polarizing sheet was placed inside the pressure vessel in front of the window through which the scattered light was collected in order to insure collection of light from only one polarization.

Pressures were measured using a manganin resistance monitored by a Wheatstone bridge. The pressures were known to 1% except at helium temperatures where corrections due to the frozen helium increased the uncertainties to (3–4)%. Temperatures in the pressure runs were not known this accurately as it was not possible to place a temperature sensor inside the cell. Instead, a carbon resistor was fastened between the pressure vessel and the cold finger, resulting in uncertainties in the measured temperature. With liquid nitrogen in the cryostat the resistor indicated a temperature of 80 K. When one makes allowances for the heat load on the pressure vessel from the pressure lines and absorbed laser light one concludes that the sample itself could have been as warm as 85 K. When liquid helium was in the cryostat the resistor indicated a temperature of 20 K. Similar considerations suggest that the sample itself may have been as warm as 30 K. We shall designate the sample temperatures as being 30 and 85 K for liquid helium and liquid nitrogen, respectively.

Temperature-dependent Raman spectra at zero pressure were obtained using a conventional gas-flow-cooled optical cryostat. A calibrated carbon resistor accurate to ± 2 K was used below nitrogen temperatures, and a thermocouple accurate to ± 2 K was used above nitrogen temperatures. Measurements were made from 7 to 300 K.

Spectra were thus obtained as functions of temperature or hydrostatic pressure. In order to intercompare these experiments it is desireable to express all spectra as functions of volume. This can be done quite easily for the temperature dependence experiments. One writes

$$\frac{V(T)}{V_0} = 1 + 3\int \alpha(T)\, dT,$$

where $V(T)$ is the volume at temperature T, V_0 is the volume at zero temperature and zero pressure, and $\alpha(T)$ is the thermal-expansion coeffi-

cient. Reliable values for $\alpha(T)$ over the temperature range of interest are easily obtained.[5]

The pressure-to-volume conversion was not as straightforward. One can presumably employ the bulk modulus β in the equation[6]

$$\frac{dV}{V} = -\frac{1}{\beta}\,dp \quad ,$$

and integrate to find $V(p)$. This procedure does not give a pressure-volume relation which agrees with the measured p-V data except at low pressures. The reason is that β is assumed to be a constant, because of the lack of experimental data giving β as a function of pressure. One expects that β should not be a constant but should stiffen with increasing pressure. At room temperature this is not a serious problem as one can employ the measured p-V data for the materials for which they are known. However, room-temperature p-V data are not available for all materials, and p-V data are not available at nitrogen and helium temperatures for any of the materials studied here. Thus, at low temperatures we were forced to calculate volumes using the bulk modulus. This result gives a one-sided systematic error in the low-temperature data by assuming the error to be equal to the difference between room-temperature p-V data and the room-temperature pressure-volume relation calculated from the bulk modulus. These one-sided error bars are shown in our results, and exceed any uncertainties in the pressure itself.

Samples were grown by the Bridgeman method

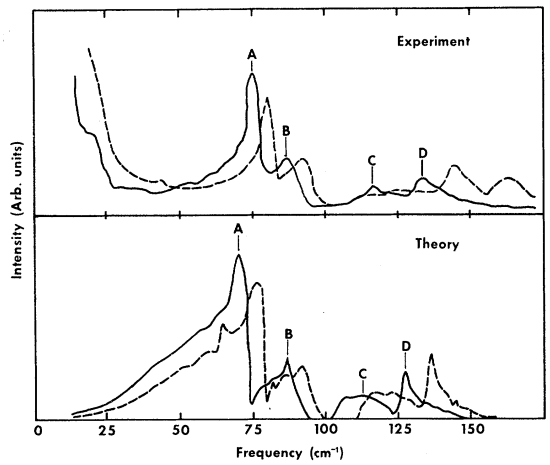

FIG. 1. Impurity-induced first-order Raman spectra of E_g symmetry in KBr:Tl$^+$. Upper: experimental spectra measured at 30 K with hydrostatic pressures of 0 kbar (solid curve) and 6 kbar (dashed curve). Lower: theoretical spectra calculated for unit cell volumes corresponding to these experimental conditions.

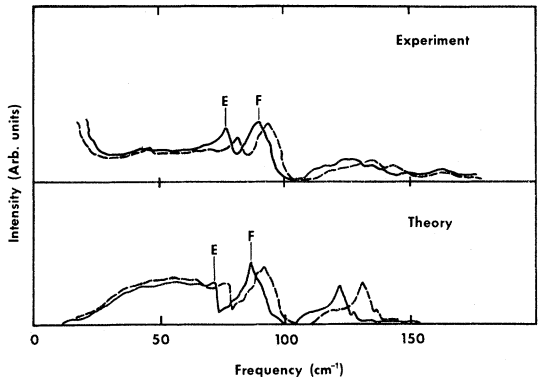

FIG. 2. Impurity-induced first-order Raman spectra of T_{2g} symmetry in KBr:Tl$^+$. Upper, experimental spectra measured at 85 K with hydrostatic pressures of 1.3 kbar (solid curve) and 6.2 kbar (dashed curve). Lower: theoretical spectra calculated for unit cell volumes corresponding to these experimental conditions.

in the Crystal Growth Laboratory at Arizona State University. Atomic absorption spectroscopic measurements showed the concentrations of Tl$^+$ to vary between 0.3 and 1.3 mol % for the samples used in this study.

III. EXPERIMENTAL RESULTS

A. Complete spectra and systematic trends

Representative data which illustrate the effects of hydrostatic pressure on the Tl$^+$-induced spectra are given in Figs. 1 and 2 for KBr:Tl$^+$.[7] These figures show the E_g spectra at 30 K for pressures of 0 and 6 kbar and the T_{2g} spectra at 85 K for pressures of 1.3 and 6.2 kbar, respectively. Both figures also show theoretical spectra which will be discussed later. The intensities of the experimental spectra have been adjusted to be approximately equal in order to facilitate comparison. Because of differing experimental conditions it is not possible to intercompare the intensities of the various spectra. In particular, pressure-dependent spectra, taken inside the pressure cell, cannot be compared with temperature-dependent spectra, taken using a simple cryostat. We have made similar arbitrary multiplicative intensity adjustments to allow comparison of experimental spectra throughout this paper.

There are several points to be noted with regard to Fig. 1. First, the spectra are continuous, extending from the tail of the stray light peak at about 30 cm^{-1} to the one-phonon cutoff near 160 cm^{-1}. Second, upon application of pressure the entire spectrum shifts to higher frequency with the higher frequency peaks shifting more than the lower frequency peaks. Third, while there are many features in the spectra, not all are real in

the sense that they can be resolved from the noise. Hence, we shall follow the behavior of only the most prominent features, namely the peaks labeled A, B, and D. Fourth, we also note the presence of a broad peak at 163 cm^{-1} in the high-pressure spectrum. The peak is not characteristic of KBr:Tl^+ since it occurs with the same shape at the same frequency in KI:Tl^+. In addition, it has no pressure dependence and is never seen in a temperature-dependence experiment, for which the pressure cell is not used. Therefore, this peak, and a similar one which sometimes occurs at 43 cm^{-1}, is an artifact of the pressure cell and is ignored here. Peak C is also excluded from the subsequent discussion because it was occasionally obscured by a laser plasma line.

One would clearly like to compare the entire experimental spectrum and its pressure dependence with the entire theoretical spectrum and its pressure dependence. The theoretical spectra shown in Fig. 1 make such a comparison possible. However, a more precise numerical comparison can be made if one compares the pressure dependence of the peaks A-D in the experimental and theoretical spectra. Throughout this paper we shall show complete representative experimental and theoretical spectra in order that the reader may assess how well they agree overall. But our discussion will be centered on the more detailed comparison of the major features in the spectra.

Experiments in which the spectrum was studied as a function of temperature at zero pressure yielded qualitatively similar results with one major exception. As noted above the spectra shifted to higher frequencies with an increase in hydrostatic pressure. For a temperature-dependence experiment the spectra shifted to *lower* frequencies with an increase in temperature. The reason for this opposite behavior is clear. Increasing pressure causes a decrease in unit cell volume, while an increase in temperature causes an increase in unit cell volume. The dominant effect of the unit cell volume can be seen in Fig. 3, where we have plotted the E_g spectrum for KBr:Tl^+ for zero pressure at 30 K and 4.2 kbars at 300 K. The temperature increase from 30 to 300 K causes a volume increase which can be calculated from the thermal-expansion coefficient. From p-V data one can in turn calculate the hydrostatic pressure which would restore the room-temperature unit cell volume to its value at 30 K and zero pressure. This value is 4.2 kbars. As can be seen in Fig. 3 the spectra coincide essentially identically, indicating the dominant influence of the unit cell volume.

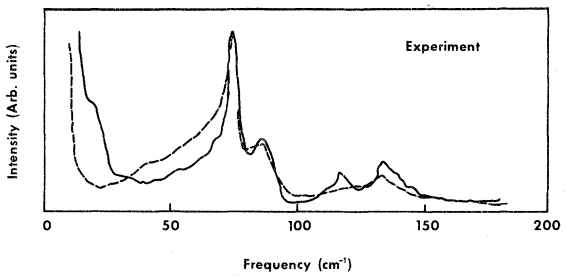

FIG. 3. E_g spectrum of KBr:Tl^+ measured at 30 K and 0 kbar (solid curve) and at 300 K and 4.2 kbar (dashed curve); the unit cell volume is the same in each of these cases.

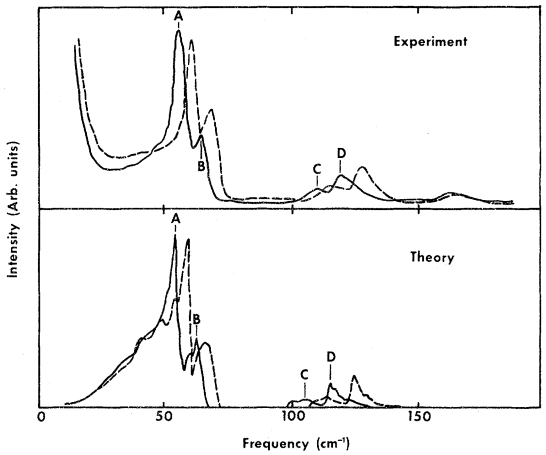

FIG. 4. Impurity-induced first-order Raman spectra of E_g symmetry in KI:Tl^+. Upper: experimental spectra measured at 85 K with hydrostatic pressure of 1.4 kbar (solid curve) and 6.9 kbar (dashed curve). Lower: theoretical spectra calculated for unit cell volumes corresponding to these experimental conditions.

Representative pressure-dependent spectra for KI:Tl^+ are shown in Figs. 4 and 5. Figure 4 shows the E_g spectra at 85 K for pressures of 1.4 and 6.9 kbar while Fig. 5 shows the T_{2g} spectra under the same conditions. In Fig. 6 we show the E_g spectra for KCl:Tl^+ at 85 K for pressures of 1.4 and 6.9 kbar, and in Fig. 7 we show the T_{2g} spectra for the same conditions. Figures 4–7 also have the prominent peaks indicated, and it is these peaks which will receive subsequent discussion. Also shown in Figs. 4–7 are the complete theoretical spectra. One can note from Figs. 1 and 2 and Figs. 4–7 that the theoretical spectra are in general in very good agreement with the experimental spectra. However, we wish to make a more careful numerical comparison of theory and experiment than these figures would allow. Accordingly, we shall now confine our attention to the various peaks labeled in the figures, and shall turn first to those conclusions

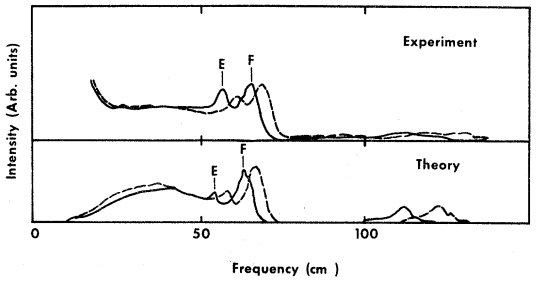

FIG. 5. Impurity-induced first-order Raman spectra of T_{2g} symmetry in KI : Tl^+. Upper: experimental spectra measured at 85 K with hydrostatic pressures of 1.4 kbar (solid curve) and 6.9 kbar (dashed curve). Lower: theoretical spectra calculated for unit cell volume corresponding to these experimental conditions.

which can be drawn from the experimental results taken alone.

B. Analysis of peak shifts

As discussed in the Introduction, one expects anharmonic interactions to produce two results, shifts in phonon frequencies, and broadening of phonon peaks. The peaks in our spectra contain contributions from many phonons and thus it is difficult to extract from our data any information on broadening of individual phonon peaks. In this first analysis it seems more useful to concentrate on the shifts of phonon peaks. Even so, each peak in the spectrum contains contributions from many phonons and as a peak shifts one is studying the net result of the shifts of these many phonons.

As we also discussed in the Introduction, one expects peak shifts to arise from two different

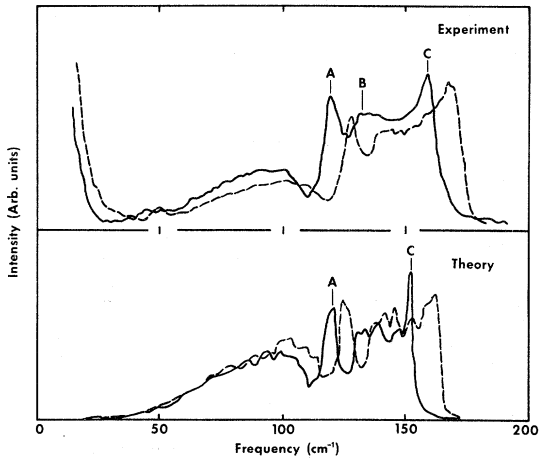

FIG. 6. Impurity-induced first-order Raman spectra of E_g symmetry in KCl : Tl^+. Upper: experimental spectra measured at 85 K with hydrostatic pressures of 1.4 kbar (solid curve) and 6.9 kbar (dashed curve). Lower: theoretical spectra calculated for unit cell volumes corresponding to these experimental conditions.

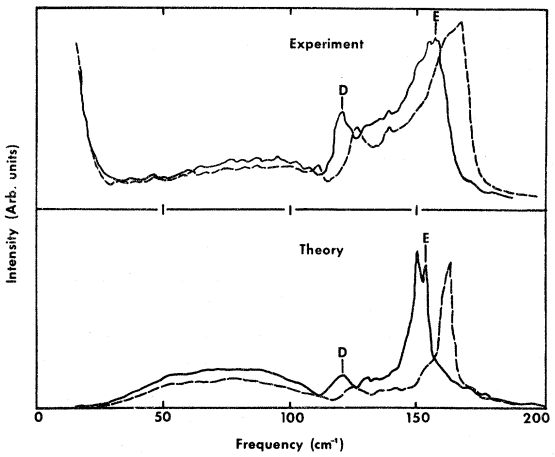

FIG. 7. Impurity-induced first-order Raman spectra of T_{2g} symmetry in KCl : Tl^+. Upper: experimental spectra measured at 85 K with hydrostatic pressures of 1.4 kbar (solid curve) and 6.9 kbar (dashed curve). Lower: theoretical spectra calculated for unit cell volumes corresponding to these experimental condtions.

manifestations of anharmonicity. The first is the volume dependence of the phonon frequencies and the second is multiphonon interactions. We wish to combine our pressure and temperature experiments to examine volume dependence and multiphonon effects separately.

We start with KBr: Tl^+. At 30 K one expects any net multiphonon contributions to the pressure dependence of peak shifts to be negligible, as one is working at about $\frac{1}{6}$ of the Debye temperature. Thus, a pressure-dependence experiment should be dominated by the volume dependence of the phonon frequencies. In Fig. 8 we show the shifts

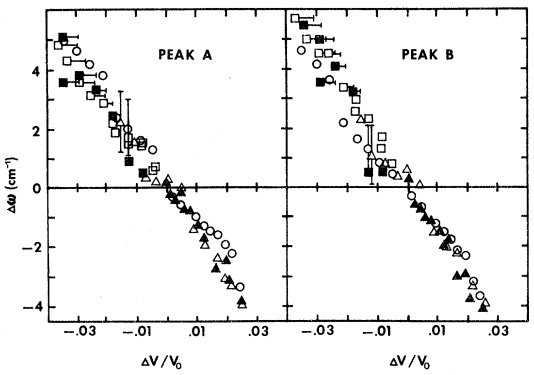

FIG. 8. Frequency shifts of peaks A and B in the E_g spectrum of KBr : Tl^+ plotted against fractional change in unit cell volume. Closed squares: pressure dependence at 30 K. Open squares: pressure dependence at 85 K. Open triangles: pressure dependence at 300 K. Closed triangles: temperature dependence at zero pressure. Open circles: shifts in calculated spectra.

in the frequencies of peaks A and B of Fig. 1 as a function of reduced unit cell volume. The frequency shift $\Delta\omega$ is defined by

$$\Delta\omega = \omega(p,T) - \omega(0,0)$$

and ΔV is defined by

$$\Delta V = V(p,T) - V(0,0) \ ,$$

where $V(0,0) \equiv V_0$ is the volume at zero temperature and zero pressure. The pressure shifts at 30 K are designated in Fig. 8 by the solid squares and the 85-K pressure shifts are designated by open squares. Uncertainties in peak position are indicated by vertical error bars, while the one-sided volume error bars show the systematic pressure-to-volume conversion problem discussed above. Also shown in Fig. 8, and designated by open triangles, are the peak shifts with pressure at 300 K. It is clear that, within the uncertainties in the data, the pressure shifts at 30 K fall on the same straight line as the pressure shifts at 85 and 300 K. Peak shifts obtained by observing the spectra as a function of temperature at zero pressure are indicated in Fig. 8 by closed triangles. It can be seen that these closed triangles lie on the same straight line as the squares and open triangles. Thus, for these two peaks, the shifts in peak position with pressure are identical to the peak shifts with temperature. We

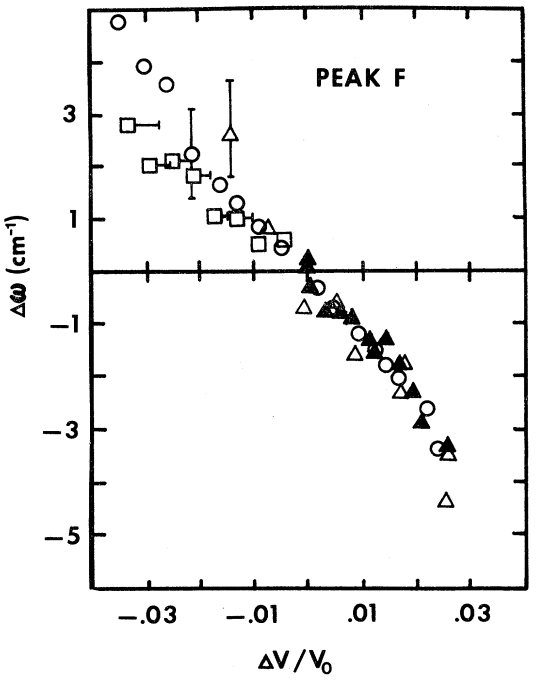

FIG. 10. Frequency shifts of peak F in the T_{2g} spectrum of KBr : Tl^+ plotted against fractional change in unit cell volume. Symbols used are the same as for Fig. 8.

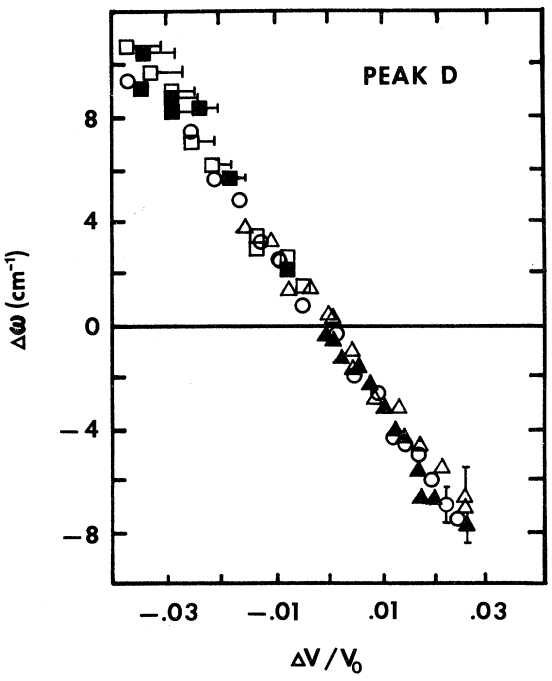

FIG. 9. Frequency shifts at peak D in the E_g spectrum of KBr : Tl^+ plotted against fractional change in unit cell volume. Symbols used are the same as for Fig. 8.

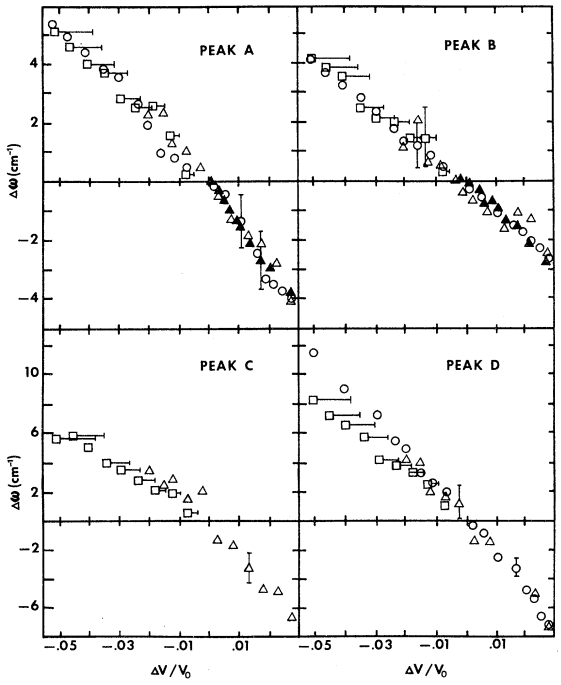

FIG. 11. Frequency shifts of peaks A, B, C, and D in the E_g spectrum of KI : Tl^+ plotted against fractional change in unit cell volume. Symbols used are the same as for Fig. 8.

shall return to this point later. The open circles in Fig. 8 are theoretical peak shifts which will also be discussed later.

Figure 9 shows the shifts for peak D in Fig. 1; the symbolism employed is the same as for Fig. 8. Thus, all of the E_g peaks studies for KBr:Tl^+ shift with pressure or temperature in the same way.

The pressure dependence of peak F in the T_{2g} spectrum of KBr:Tl^+, (Fig. 2) is shown in Fig. 10. The symbols used are the same as for Fig. 8.

In sum, the E_g and T_{2g} spectra for KBr:Tl^+ show the following systematic behavior. Shifts of peaks A, B, D, and F with pressure at 30 K fall on the same straight line as shifts of the same peaks with pressure at 85 and 300 K. Shifts with temperature at zero pressure fall on the same straight line as the pressure shifts.

Pressure and temperature shifts of peaks A-D of the E_g spectrum for KI:Tl^+ are shown in Fig. 11, while the shifts of peaks E and F of the T_{2g} spectrum are shown in Fig. 12. Again, the open squares indicate the pressure dependence at 85 K, the open triangles indicate the pressure dependence at 300 K and the temperature dependence at zero pressure is given by the closed triangles. Open circles again are theoretical shifts which will be discussed later.

It is evident that all three experiments (pressure dependence at 85 and 300 K and temperature dependence at zero pressure) yield peak shifts which fall on the same straight line. One notes that the one-sided error bars for the pressure-to-volume conversion at 85 K are very large for KI, illustrating the large disparity between the p-V data and a bulk modulus calculation of a p-V curve. The straight-line fit to the three experiments is improved if one selects the right-handed end of the volume error bars at 85 K.

Pressure and temperature shifts for the E_g peaks A-C in the KCl:Tl^+ spectra are shown in Figs. 13 and 14, while the shifts for the T_{2g} peaks E and F are shown in Fig. 15. The symbols are the same as for KI:Tl^+. Volume errors at 85 K are about half as great for KCl as for KI. Within the uncertainties of the data the best fits for peaks A-E are straight lines which connect the pressure and temperature shifts on the same lines.

The same systematic behavior is observed for KCl, KBr, and KI doped with Tl^+. In all cases the pressure shifts of the strongest spectral features and the temperature shifts of the same features fall on the same straight line relating frequency shift to reduced unit cell volume. As argued above, one expects that the pressure experiments at low temperatures would give frequency shifts dominated by the volume dependence of the force constants. One might also expect pressure experiments at high temperatures and temperature experiments at zero pressure to give frequency shifts due both to the volume dependence of the force constant and to multiphonon interactions. The fact that all

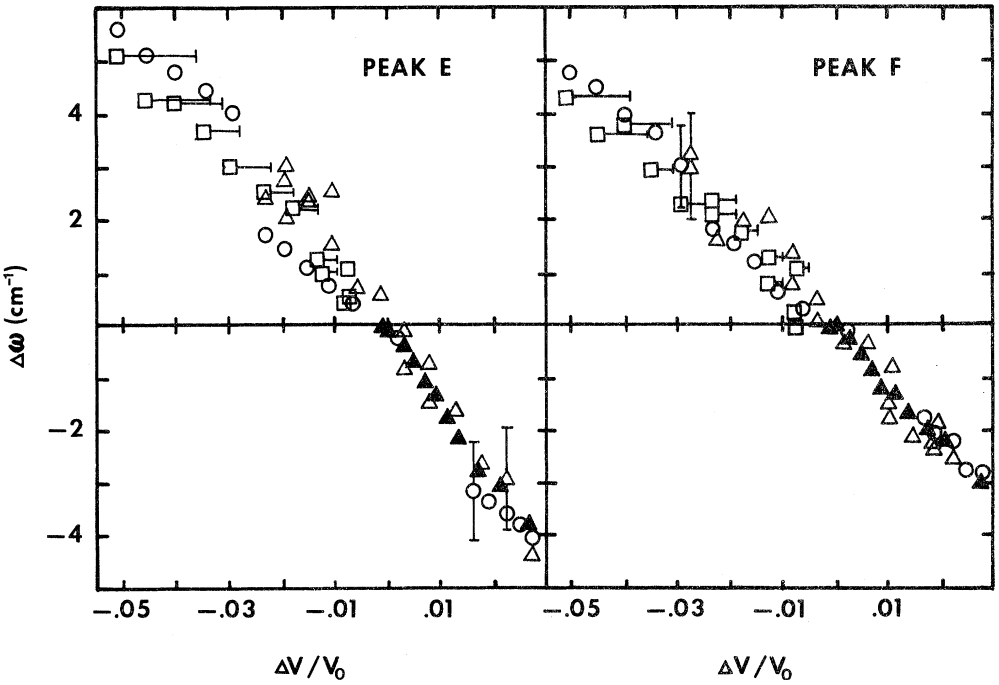

FIG. 12. Frequency shifts of peaks E and F in the T_{2g} spectrum of KI:Tl^+ plotted against fractional changes in unit cell volume. Symbols used are the same as for Fig. 8.

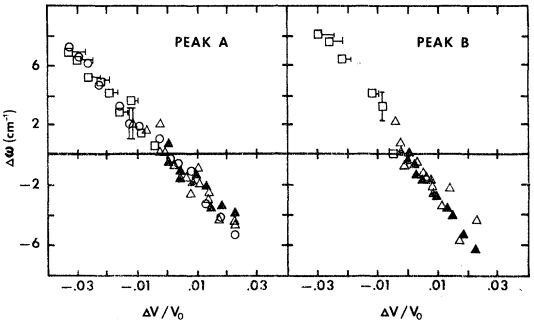

FIG. 13. Frequency shifts of peaks A and B in the E_g spectrum of KCl : Tl^+ plotted against fractional change in unit cell volume. Symbols used are the same as for Fig. 8.

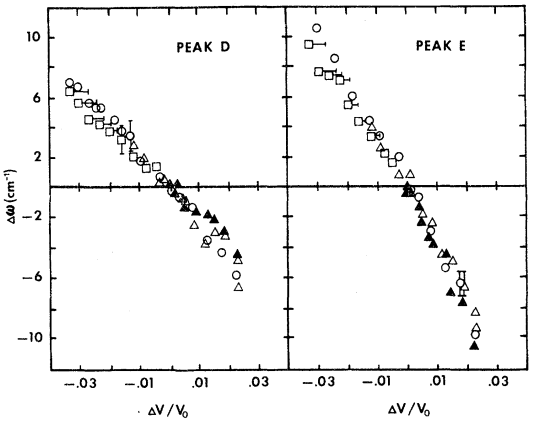

FIG. 15. Frequency shifts of peaks D and E in the T_{2g} spectrum of KCl : Tl^+ plotted against fractional change in unit cell volume. Symbols used are the same as in Fig. 8.

shifts are found to lie on the same straight line when plotted as a function of reduced unit cell volume leads us to conclude that it is the volume dependence of the force constants which is the dominant effect in all three systems.

One might inquire as to whether there is some systematic feature of our experimental approach which precludes the observation of multiphonon effects. The answer is that we have occasionally observed results which can be interpreted as due to multiphonon interactions, as exemplified in Fig. 16. Here we have plotted the volume dependence of the frequencies of the peaks D and E of the T_{2g} spectra of KCl:Tl^+, for both pressure and temperature experiments. Note that we have plotted here the frequency of the peak rather than the shift in the frequency of the peak. Peaks D and E behave very differently. For peak D the peak frequency itself has the same linear dependence on unit cell volume for both pressure experiments and for the temperature experiment. Peak E, however, has a frequency which depends linearly on unit cell volume for a pressure experiment at 85 K while the frequency falls on a different straight line for a pressure experiment at 300 K. These two lines are parallel, with the result that plots of frequency shifts for these two experiments will fall on a single straight line, as in Fig. 15. In addition, the volume dependence of the peak frequency for peak E as determined by a temperature-dependence experiment is seen in Fig. 16

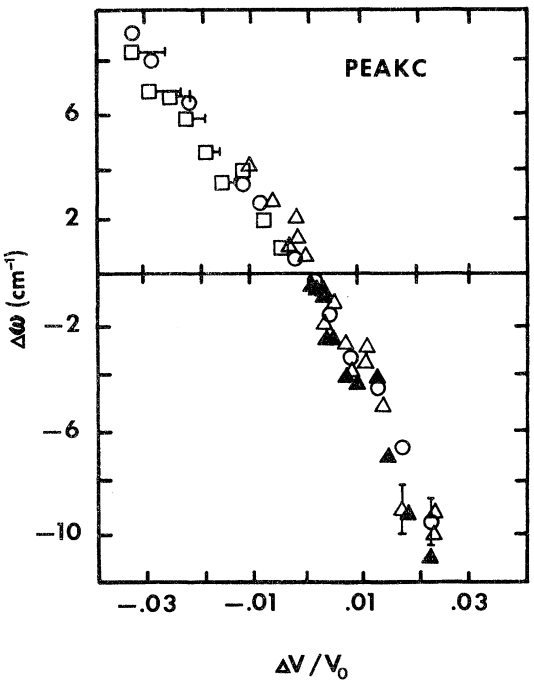

FIG. 14. Frequency shifts of peak C in the E_g spectrum of KCl : Tl^+ plotted against fractional change in unit cell volume. Symbols used are the same as for Fig. 8.

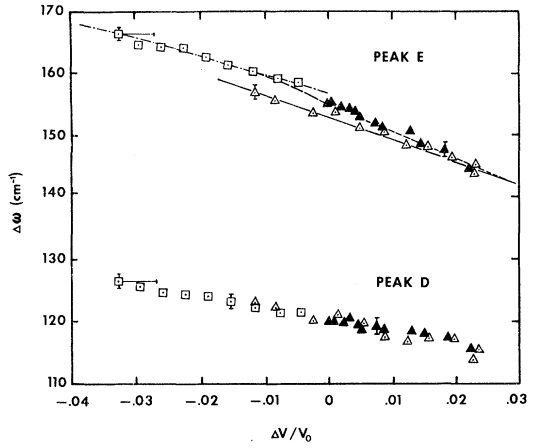

FIG. 16. Frequencies of peaks D and E in the T_{2g} spectrum of KCl : Tl^+ plotted against fractional change in unit cell volume. Symbols used are the same as in Fig. 8.

to be one which connects the two different pressure experiments. Again, when one plots shifts in frequency for the temperature-dependence experiment the result will be on essentially the same line as the pressure experiment, if allowance is made for all error bars. This can also be seen in Fig. 15. However, Fig. 16 suggests that the three different experiments give volume dependences of the peak frequency which are marginally outside the experimental error, and are therefore different. The reason for these differences would presumably be multiphonon interactions. If one invokes multiphonon effects for peak E in Fig. 16, one can conclude that their volume dependence is merely a constant at constant temperature. Of all the peaks discussed here only the peak E in the T_{2g} spectrum for KCl so clearly shows possible multiphonon effects.

The experimental results can be summarized, then, by stating that for all three hosts the dominant effect in both the pressure and temperature-dependence experiments is that the shifts of peak in the first-order spectrum are functions of just the unit cell volume. This implies that the dominant underlying anharmonic mechanism is the volume dependence of the force constants which determine the phonon frequencies. These experimental conclusions will be substantiated and extended by the results of the theoretical calculations, to which we now turn.

IV. THEORY

The theoretical calculations of the volume-dependent Raman spectra of Tl^+-doped potassium halides proceed in two steps.

The first of these involves the calculation of the host crystal phonons for a given volume within the framework of a quasiharmonic model, the details of which have been discussed elsewhere.[8] Briefly, it consists of starting with bare harmonic phonons given by the breathing shell model[9] (BSM), whose input parameters are appropriate to the host crystal at 0 K and zero pressure.[10] The volume change of the crystal is described in terms of a linear homogeneous strain, which modifies the bare harmonic force constants by means of terms involving third-order anharmonicities in the potential energy. These are assumed to be derivable from a central potential acting between just nearest neighbors. This assumption leads to two independent anharmonicity parameters, one of which is obtainable from the harmonic force constants of the breathing shell model. The single remaining anharmonicity parameter is gotten by fitting the observed thermal-expansion coefficient[11,12] over the temperature range 20–300 °K. Details and numerical values are provided in Ref. 8, where an alternative procedure for obtaining the anharmonicity parameters from a Born-Mayer potential is discussed and is shown to lead to poor results for the temperature dependences of the reststrahlen frequencies and dielectric properties of pure KCl, Br, and KI. This alternative procedure was also used in computing the volume-dependent Raman spectra. Here too it leads to significantly worse results than does the thermal-expansion fit described above, and it will not be considered further. With the anharmonicity parameters determined, the quasiharmonic phonons, which are those corresponding to the changed volume of the crystal, are calculated using first-order perturbation theory.

The second step is the calculation of the defect-induced first-order Raman spectra using the quasiharmonic phonons. The general procedure used for computing off-resonance spectra of Tl^+-doped alkali halides is discussed in HPW. In that paper the dominant electron-phonon coupling was assumed to be linear in the displacements of the defect's nearest neighbors, and the resulting theoretical calculations were in excellent agreement with experiment for the acoustic region of the spectra. For the potassium halides, however, experimental peaks in the optical regions were not well described. Robbins and Page,[13] have recently shown that very good agreement with the entire experimental spectra of Tl^+-doped KCl, KBr, and KI can be obtained by assuming the electron-phonon interaction to be linear in the displacements of the defect's second-nearest as well as nearest neighbors, and we have used the formalism of Ref. 13 to compute the volume dependence of the Raman spectra. The inclusion of second-neighbor contributions to the electron-phonon coupling introduces two parameters which are functions of the electronic polarizability derivatives with respect to displacements of the defect's first- and second-nearest neighbors. In this work we have employed the values of these parameters given in Ref. 13.

As discussed in Refs. 1 and 13, the best agreement between theory and experiment for the $T=0$ zero-pressure spectra of KI:Tl^+ and KBr:Tl^+ was obtained for the case of no defect-induced force-constant perturbations. Accordingly, defect-induced force-constant perturbations are assumed to be zero for these systems in the present work. For KCl:Tl^+, on the other hand, it was shown in Ref. 1 that the best agreement for the $T=0$ zero-pressure E_g spectrum was obtained for a 10% stiffening of the defect-nearest-neighbor longitudinal force constants, and the present calculations are based upon this model.[14] The T_{2g} spectrum is unaffected by this perturbation. Moreover, since the Raman-active modes are of even parity and therefore involve no defect motion, they are unaffected by the large mass perturbation intro-

duced by the thallium ion. Hence the Raman spectra of the systems studied here reflect the unperturbed (or very weakly perturbed in the case of the E_g phonons in KCl:Tl^+)host crystal phonons.

The quasiharmonic projected densities of states needed for computing the first-order Raman spectra were obtained in the same manner as the corresponding $T=0$ zero-pressure quantities of Refs. 1 and 13, except that the quasiharmonic phonons were used. The projected densities were computed as histograms of 100 bins of equal width over the squared frequency range of the quasiharmonic phonons, and the bin's midpoints were connected by straight-line segments. The calculations involved summations over 1686 wave vectors in the $\frac{1}{48}$ irreducible element of the Brillouin zone, which corresponds the inclusion of 64 000 wave vectors in the entire zone.

V. NUMERICAL CALCULATIONS AND DISCUSSION

A. KI:Tl^+

The calculated E_g and T_{2g} spectra of KI:Tl^+ for two different volumes are shown in Figs. 4 and 5, respectively, underneath the corresponding experimental spectra. The calculated and experimental spectra are in good agreement not only in general appearance and relative intensities of the peaks, but also with regard to the manner in which the spectra shift to higher frequencies as the crystal volume is reduced. Note that although the positions of the major peaks A, B, C, and D in the calculated E_g spectra and peaks E and F in the calculated T_{2g} spectra are generally not in exact coincidence with the corresponding experimental peaks, the frequency shifts of the peaks appear to be in good agreement. We now consider in detail the frequency shifts of these peaks as a function of the crystal's volume change.

Figure 11 shows the shifts of peaks A, B, C, and D of the E_g spectrum as a function of the fractional volume change of the crystal. The shifts $\Delta\omega$ are taken with respect to the peak positions for 0 K and zero pressure. Likewise, ΔV denotes the volume change with respect to V_0, the volume at 0 K and zero pressure.

As discussed in Sec. II, different sets of experimental data are given in Figs. 11 and 12. Open squares represent the pressure dependence measurements at 85 K, open triangles indicate the pressure-dependence measurements at 300 K and the zero-pressure temperature-dependence measurements are given by closed triangles. Theoretical shifts are denoted by open circles.

Since the position of a theoretical peak is known only to within the width of its histogram bin, theoretical error bars corresponding to this width are given. An additional source of theoretical uncertainty arises from the fact that the maximum quasiharmonic phonon frequency may have a different volume dependence than the peak under consideration. Since the bin boundaries are determined by ω_{max}, this behavior can result in a peak position "jumping" from one bin to its neighbor for a very small volume change.

For peaks A and B, it is noted that all four sets of shifts are in very good agreement with each other. As argued previously the fact that the three experimental sets agree with each other indicates that the observed shifts are purely volume dependent; multiphonon contributions to the shifts, which exist in principle in the temperature-dependence measurements, are too small to be detected. Moreover, the good agreement between the theoretical and experimental shifts, together with the fact that just pure KI anharmonicities were used in the calculations, leads to the conclusion that the observed shifts are the result of anharmonicity in pure KI.

Turning now to the optical peaks C and D, we note that no temperature-dependence measurements are available for them. Moreover, as can be seen in the calculated spectra of Fig. 4, peak C was found to be so broad that its calculated shift could not be accurately determined. For peak D, the calculated and measured shifts are in agreement within the joint theoretical and experimental uncertainties.

The shifts of the T_{2g} peaks E and F are given in Fig. 12. For these peaks the shifts obtained from all three sets of measurements are in very good agreement with each other and with the calculated shifts.

B. KBr:Tl^+

The calculated E_g and T_{2g} spectra for KBr:Tl^+ are given for two different volumes in Figs. 1 and 2. Calculated E_g spectra for these two volumes were presented in a preliminary report,[7] of this work, where the HPW assumption of an electron-phonon coupling involving just the defect's nearest neighbors was used. Therefore in that work the peaks C and D, which according to Ref. 13 result from the second-neighbor contributions to the electron-phonon interaction, were not obtained. Note that both the E_g and T_{2g} spectra are qualitatively similar to those for KI:Tl^+.

In Figs. 8 and 9, the frequency shifts for the E_g peaks A, B, and D of Fig. 1 are shown. Recall that we are not following peak C since it was sometimes obscured by a laser plasma line in the experiments. In addition, to the three sets of measurements as discussed for KI:Tl^+, Figs. 8 and 9 also show the results of pressure-dependence experiments done at 30 K. These are indicated by the closed squares. The shifts of peaks A and B were previously discussed in Ref. 7, and

we note in passing that all four sets of measurements and the calculated shifts are in very good agreement. For peak D, one again sees that there is excellent agreement between all four sets of measurements and the theoretical shifts.

The shifts of the T_{2g} peak labelled F in Fig. 2 are plotted in Fig. 10. No measurements of the T_{2g} spectra were done at 30 K, so that there are three sets of measured shifts for peak F. Again within the joint experimental and theoretical uncertainties, the calculated and measured shifts are in good agreement. Note that for KBr, the uncertainties in the volume determination at low temperatures are less than they were for KI.

C. KCl:Tl$^+$

The computed spectra for this system are given for two different volumes in Figs. 6 and 7. The shifts of the E_g peaks A, B, and C are plotted in Figs. 13 and 14. The symbols have the same meaning as for KI:Tl$^+$. Peak B could not be unambigously determined in the calculated spectra, and hence calculated shifts are not plotted for this peak. Again, the different sets of experimental shifts for each peak are in good agreement with each other, and the agreement between theory and experiment for the shifts of peaks A and C is very good. Recall that in contrast to the calculated spectra for KI:Tl$^+$ and KBr:Tl$^+$, the calculated E_g spectrum of KCl:Tl$^+$ was based upon a 10% force constant stiffening. Nevertheless, only pure crystal anharmonicities were used in the calculations of the shifts, and the good agreement between theory and experiment again leads to the conclusion that the measured shifts are determined by anharmonicity in pure KCl.

The shifts of the T_{2g} peaks E and F are plotted in Fig. 15. For each peak, the three sets of measurements and the calculated shifts are in good agreement within the joint uncertainties.

We recall that when the volume dependence of peak E's frequency, rather than its frequency shift, is plotted as in Fig. 15, a possible small multiphonon contribution of ~ 3 cm^{-1} that appears to be volume independent at a fixed temperature, is indicated. Such a multiphonon contribution cannot, of course, manifest itself in the peak shifts and thus does not appear in Fig. 14. As discussed earlier, this peak provides the clearest indication of possible multiphonon effects in the present work, but even for this peak the identification is marginal, owing to the experimental uncertainties. At any rate, multiphonon effects make little or no contribution to the shifts of any of the peaks studied in this paper, and in all cases good agreement between the theoretical and experimental shifts is obtained by assuming that the shifts arise from anharmonicity in just the pure host crystal.

VI. SUMMARY AND CONCLUSIONS

Our measurements have shown that the frequency shifts of the most prominent spectral features for all three systems under study here can be accounted for almost exclusively by variations in the unit cell volume. Frequency shifts obtained from temperature-dependence and frequency-dependence measurements all fall on the same straight line (allowing for experimental uncertainties) when plotted against reduced unit cell volume. We conclude that the volume dependence of the pure crystal harmonic force constants is the dominant anharmonic effect in these systems, and that the net contribution to frequency shifts from multiphonon interactions is negligible. In the one instance encountered here where multiphonon effects may be significant (peak E in the T_{2g} spectrum of KCl:Tl$^+$, Fig. 16), the result was a small volume-independent contribution to the phonon frequencies.

These conclusions have been supported by our calculations of the volume dependence of the Tl$^+$-induced first-order spectra using unperturbed (or, in the case of the E_g spectra of KCl:Tl$^+$, weakly perturbed) BSM phonons and pure crystal anharmonicity in a quasiharmonic model. Similar calculations have previously been shown to give excellent reproductions of the measured spectra at zero pressure and 0 K.[1] The calculations reported here extend the earlier results to higher temperatures and pressures; they lead to frequency shifts which are in agreement with the measured shifts for all of the spectral features studied here. Again, we are led to conclude that multiphonon processes produce a negligible contribution to the frequency shifts in these systems.

---

*Work supported by the NSF under Research Grant No. GH34248.

†Present address: Department of Natural Sciences, University of Michigan, Dearborn, Mich. 48128.

[1]R. T. Harley, J. B. Page, Jr., and C. T. Walker, Phys. Rev. B 3, 1365 (1971).

[2]Prelininary reports on this work have been presented: J. Potts and C. T. Walker, Bull. Am. Phys. Soc. 18, 370 (1973); J. A. Taylor and C. T. Walker, *ibid.* 19, 105 (1974); M. S. Haque and J. B. Page, Jr., Bull. Am. Phys. Soc. 19, 652 (1974).

[3]D. B. Fitchen, Rev. Sci. Instrum. 34, 673 (1973).

[4]J. S. Dugdale, Nuovo Cimento Suppl. 9, 27 (1958).

[5]*American Institute of Physics Handbook*, 3rd Ed., edited by D. E. Gray (McGraw-Hill, New York, 1972), pp. 4–49.

[6]Duane Wallace, *Thermodynamics of Crystals* (Wiley, New York, 1972), pp. 468–9; and Ref. 5, pp. 4–137.

[7]A preliminary report of the results for KBr : Tl^+ has appeared in the literature: J. A. Taylor, M. S. Haque, J. E. Potts, J. B. Page, Jr., and C. T. Walker, Solid State Commun. 16, 1179 (1975).
[8]M. S. Haque, Phys. Rev. B 12, 1501 (1975).
[9]U. Schröder, Solid State Commun. 4, 347 (1956).
[10]J. B. Page, Jr. and D. Strauch, Phys. Status Solidi 24, 569 (1967).
[11]G. K. White, Proc. R. Soc. A 286, 204 (1965).
[12]B. Yates and C. H. Panter, Proc. Phys. Soc. Lond. 80, 373 (1962).
[13]D. Robbins and J. B. Page, Jr., Bull. Am. Phys. Soc. 19, 105 (1974); and (to be published).
[14]Robbins and Page (Ref. 13) have shown that the observed peak at 159 cm^{-1} in the E_g spectrum of KCl : Tl^+ (peak *C* of Fig. 6) can be well-accounted for in terms of second-neighbor contributions to the electron-phonon interaction as discussed just previously or in terms of a slight (< 10%) stiffening of the longitudinal force constants between the impurity's first- and fourth-nearest neighbors. Such stiffening would arise from a small outward distortion of the lattice around the defect. The results of Ref. 13 in fact point to the likelihood of both mechanisms being important for this peak. Since the effect of either mechanism is to introduce contributions from the K^+ ions to the calculated projected density of states, it is unlikely that the volume dependence of the 159-cm^{-1} peak would differ for the two mechanisms, and in this paper we have neglected force constant changes beyond the defect's nearest-neighbors for KCl : Tl^+.